Detection of Fecal Residue on Poultry Carcasses by Laser-Induced Fluorescence Imaging

B. Cho, M.S. Kim, K. Chao, K. Lawrence, B. Park, and K. Kim

ABSTRACT: Feasibility of fluorescence imaging technique for the detection of diluted fecal matters from various parts of the digestive tract, including colon, ceca, small intestine, and duodenum, on poultry carcasses was investigated. One of the challenges for using fluorescence imaging for inspection of agricultural material is the low fluorescence yield in that fluorescence can be masked by ambient light. A laser-induced fluorescence imaging system (LIFIS) developed by our group allowed acquisition of fluorescence from feces-contaminated poultry carcasses in ambient light. Fluorescence emission images at 630 nm were captured with 415-nm laser excitation. Image processing algorithms including threshold and image erosion were used to identify fecal spots diluted up to 1:10 by weight with double distilled water. Feces spots on the carcasses, without dilution and up to 1:5 dilutions, could be detected with 100% accuracy regardless of feces type. Detection accuracy for fecal matters diluted up to 1:10 was 96.6%. The results demonstrated good potential of the LIFIS for detection of diluted poultry fecal matter, which can harbor pathogens, on poultry carcasses.

Keywords: fecal residues, fluorescence imaging, food safety, laser induced, poultry carcasses

Introduction

Ensuring safety of food commodities is a current issue of major importance in the meat industry. Consumption of poultry contaminated with feces can cause serious human illness (Cody and others 1999; Mead and others 1999). Thus inspection regulations of the Food Safety and Inspection Service (FSIS) of the U.S. Dept. of Agriculture (USDA) include a zero-tolerance policy for visible fecal contaminants on poultry products (FSIS 2004).

Common routes of poultry skin contamination are ruptures of the digestive tract during evisceration process that can expel internal content. Even though a human expert inspects the wholesomeness of carcasses on the processing line, trace or dilute fecal contaminants may not be easily discernable from water and skin by the human eye. Previous research has shown potential of multispectral reflectance imaging techniques for detection of fecal matters on poultry carcasses (Park and others 2002, 2005). Results demonstrated that feces residues on poultry carcasses could be detected with approximately 92.5% accuracy using band ratio of images at 565 and 517 nm; however, efforts still need to be made to improve the detection sensitivity for the diluted fecal contaminants to comply with zero-tolerance standards for contaminant-free production.

Recent research conducted at the ARS Food Safety Laboratory (FSL) in Beltsville, Md., U.S.A. exhibited that fluorescence is very sensitive in detecting animal feces on agricultural commodities (Kim and others 2003a, 2003b, 2008). The researchers indicated that multispectral imaging using 2 to 3 fluorescence emission bands was sufficient to detect animal feces on apples. To accomplish fluorescence imaging under ambient lighting conditions, we developed a gated system capable of nano-second (ns) scale time-resolved fluorescence imaging utilizing a tunable pulsed laser to provide proper excitation.

In this study, the feasibility of a laser-induced fluorescence imaging technique is explored for the detection of diluted poultry feces on poultry carcasses. Optimal discrimination parameters, such as gate-delay time, threshold of fluorescence intensity, and image processing algorithm were suggested.

MS 20080992 Submitted 12/8/2008, Accepted 1/16/2009. *Author Cho is with Bioindustrial Machinery Engineering Dept., Chungnam Natl. Univ., 220 Gung-dong, Yuseong-gu, Daejeon, 305-764, Republic of Korea. Authors Kim and Chao are with Food Safety Laboratory, Animal and Natural Resources Inst., Agricultural Research Service, U.S. Dept. of Agriculture, Powder Mill Rd., Building 303, BARC-East, Beltsville, MD 20705, U.S.A. Authors Lawrence and Park are with Quality and Safety Assessment Unit, Richard B. Russell Agricultural Research Center, Agricultural Research Service, U.S. Dept. of Agriculture, 950 College Station Rd., Athens, GA 30605, U.S.A. Author Kim is with Center for Environment & Safety Measurement, Korea Research Inst. of Standards and Science, 1 Doryong-dong, Yuseong-gu, Daejeon, 305-340, Republic of Korea. Direct inquiries to author Cho (E-mail: chobk@cnu.ac.kr).*

Materials and Methods

Sample materials

The carcasses and digestive tracts of 15 chickens, which were grown on soybean protein meal using standard practices until slaughter at the age of 7 wk, were obtained from a poultry processing plant in Cordova, Md., U.S.A. Feed and water were withheld for 10 h prior to the slaughter. The samples were placed in plastic bags, covered with ice, and transported to the laboratory within 2 h. Fecal matter from 4 different parts of the digestive tracts, colon, ceca, small intestine, and duodenum were extracted and diluted 1:5, 1:10, and 1:50 by weight with double-distilled (DD) water. Note that diluted fecal mixtures contained particulates and no attempts were made to dissolve the particulates; however, particulates tended to aggregate toward the middle, and thus the mixtures were gently stirred prior to application on the poultry skin. Using a pipette with approximately 2-mm section of the tip removed to accommodate particulates, undiluted and diluted fecal samples were applied in 50 μL drops to the surface of the poultry carcasses. The mean dry matter contents (with standard deviations in parentheses) of ceca, small intestine, and duodenum were 180 (21), 161 (21), and 149 (18) μg/g, respectively. Note that the dry matter content for colon could not be measured owing to insufficient sample quantity.

doi: 10.1111/j.1750-3841.2009.01103.x

THE Society for Food Science & Technology
Journal of Food Science
A Publication of the Institute of Food Technologists

Measurement of fluorescence spectra

Fluorescence characteristics of poultry fecal and organic matters (skin and meat) were investigated with a spectrofluorometer (Fluorolog III, Horiba Industries, Edison, N.J., U.S.A.) with additive-dispersion double grating and 2 Czerny-Turner double monochromators. One monochromator is attached to a 450 W xenon lamp with variable excitation from 220 to 700 nm. The other is attached to a photon counting photomultiplier tube (PMT) capable of acquiring fluorescence emissions from 250 to 900 nm. The system monitors the lamp intensity through a beam splitter with a photon detector and corrects for fluctuations in lamp intensity.

Emission spectra were acquired at 2-nm intervals from 370 to 750 nm with excitation wavelengths at 5-nm increments from 350 to 610 nm. Monochromator slit widths of 2 nm were set for both of excitation and emission with the PMT integration time of 0.1 s. After construction of fluorescence emission–excitation matrices for samples, emission spectra at the excitation maximum wavelength and excitation spectra at the emission maximum wavelength for samples were measured at 1-nm intervals to refine optimal excitation and emission wavelengths. The optimized excitation and emission wavelengths were used for constructing the laser-induced fluorescence imaging system.

Laser-induced fluorescence imaging system (LIFIS)

A schematic diagram and a photo of the LIFIS is shown in Figure 1. It consists of a tunable laser, a beam expander, a C-mount zoom lens, a common aperture adapter, and a fast-gated intensified CCD camera. The excitation laser is a frequency tripled, Nd:YAG laser (10 Hz, 6-ns pulse width) with high pulse energy emitting from 410 to 690 nm (Vibrant VIS, Opotek, Calif., U.S.A.). The 6-mm-dia laser beam was expanded using a pair of divergent lenses to illuminate whole chicken carcasses under investigation at a distance of about 150 cm from the laser. A fast nanosecond-scale gated-intensified CCD camera (Istar, Andor Technology, Mass., U.S.A.) coupled to a C-mount 25-mm lens (Rainbow, Calif., U.S.A.) and a common aperture multispectral adapter (MSAI-04, Optical Insights, Ariz., U.S.A.) was used to collect fluorescence emission. The adapter uses prisms to convert the incoming image into 4 equally sized images in separate quadrants of the focal plane of the camera. Interference filters can be inserted into the aperture for multispectral imaging.

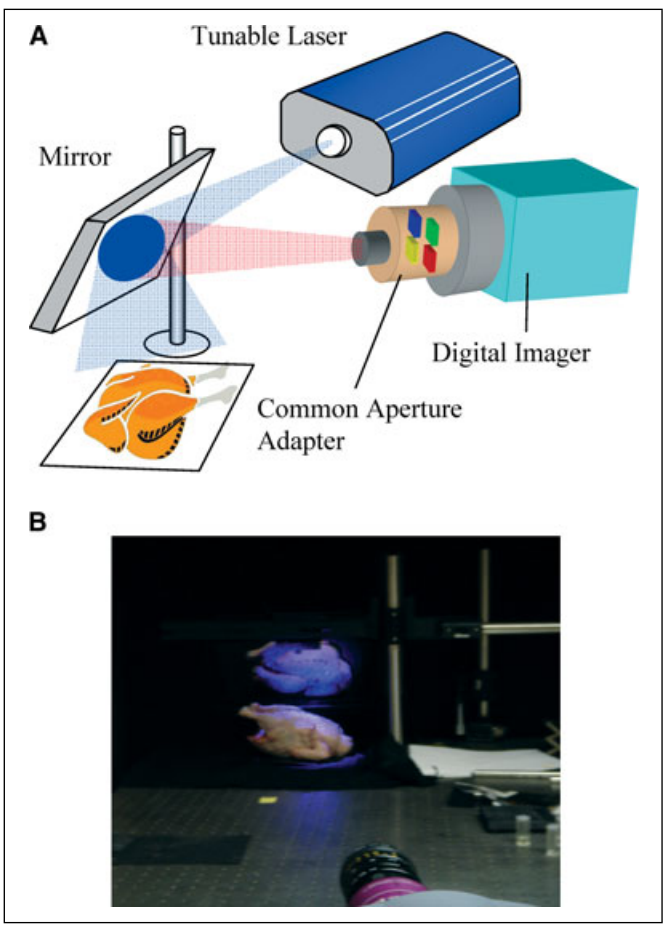

Figure 1 — Schematic (A) and a photo (B) of the LIFIS.

Image acquisition and processing

Visual Basic software (version 6.0, Microsoft, Seattle, Wash., U.S.A.) operating in a MS Windows environment was used to control the imaging system and to acquire image data (512 × 512 pixel). Images were stored as 16-bit signed integers in a sequential binary file. Fifty time-resolved images spanning 50 ns with approximately 1-ns gate width were acquired for each sample. To minimize the variability inherent in using a pulse laser, responses at individual times were averaged over 16 pulses; averaging kept pulse energy variations between time scales to less than 0.5%. Initial system gate-delay time was chosen such that no fluorescence emission from the sample was detected; this image was used for dark current and subtracted from the rest of the images. Energy output of the laser was adjusted to 20 mJ/pulse. However, due to the expansion of the laser beam, the total energy delivered to the target per unit area was less than 2 mJ/mm^2. Under this condition, no property change could be observed in the sample materials.

Image processing was performed for the acquired image data using Matlab software (version 7.0.4, The Mathworks, Natick, Mass., U.S.A.). Selection of optimal gate-delay time was based on F values of analysis of variance (ANOVA) for relative fluorescence intensity (RFI) values of respective gate-delay time between skin and fecal groups. The optimal threshold value of RFI at which the classification accuracy was highest was determined by investigating iterative threshold increments of 0.1% RFI.

Results and Discussion

Three-dimensional fluorescence excitation and emission contour plots for poultry skin and feces were constructed using a spectrofluorometer as shown in Figure 2. The most dominant fluorescence feature of the poultry feces was an emission peak in the red region of the spectrum at about 635 nm with excitation in the blue region (410 to 415 nm) while no apparent emission peak was found in the red region for the poultry skin. Selection of wavelengths and bandwidths of the filters was based on the typical emission characteristics of poultry fecal matter (Figure 3).

To refine optimal excitation and emission wavelengths for the detection of poultry feces, spectra were measured at 1-nm intervals with the excitation monochromator positioned at the excitation wavelengths previously identified as eliciting maximal responses (411 nm); subsequently, excitation spectra were measured with the PMT positioned at the maximal wavelengths identified with the 1-nm interval emission scans (Figure 3). Excitation maxima (peaks) were observed at 411 nm. The excitation spectra for 635- and 692-nm emission maxima exhibited similar characteristics.

Figure 4A shows representative emission spectra of poultry feces and organic matters resulting from excitation at 411 nm. Emission maxima were observed at 580, 625, 635, and 692 nm. The peak fluorescence response of feces is probably directly related to chemical compounds in the feedstuffs and its metabolites produced in the poultry digestive tract; however, the effects of animal digestive processes on feedstuffs were not defined explicitly so far. Kim and others (2003b) proposed that Protoporphyrin IX is a major constituent found in poultry feces that can affect the spectra shapes. Among the emission maxima, fluorescence intensities at 635 nm exhibited relatively greater differences between the feces and organic matters (Figure 4B).

Excitation at 415 nm and emission band at 635 nm were considered for this investigation, and narrow interference filter (10-nm full width at half maximum) centered at 630 nm were selected for LIFIS. The laser is capable of providing excitation at from 410 nm; however, 415 nm was selected to avoid unstable performance of the light source at the extremes of the operating wavelength range. Note that the selection of the emission filters was limited by commercial availability.

Representative ns-scale time-resolved fluorescence emission spectra of poultry feces and skin are shown in Figure 5. The fluorescence peak intensity for the feces and skin was observed at 14 ns. In general, fluorescence responses of untreated feces were greater than responses for skin and diluted fecal matters. However, some scattered spots in the areas for skin showed high fluorescence responses which were greater than responses of diluted fecal matters. A possible explanation for the high fluorescence response of the spots may be the presence of feather roots remaining in skin pores.

Figure 6 illustrates time-resolved fluorescence images spanning from 10 to 50 ns in 5-ns intervals for a poultry carcass artificially contaminated with the diluted and undiluted feces. These images were normalized to the peak intensity. Most of the images showed

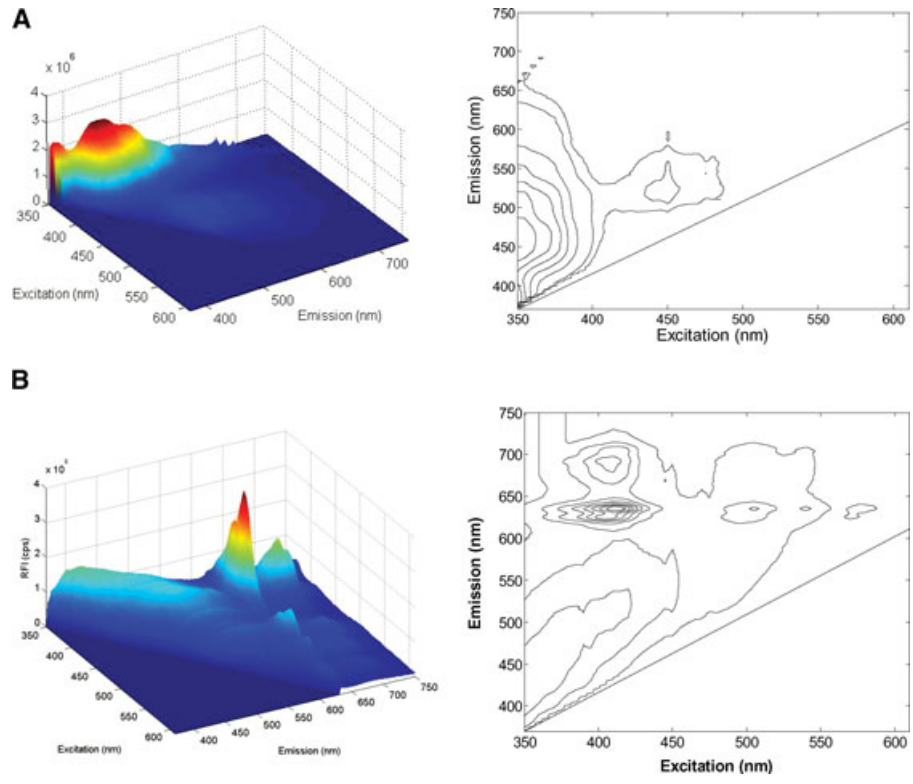

Figure 2—Representative fluorescence excitation and emission characteristics of poultry skin (A) and fecal matter from the ceca (B).

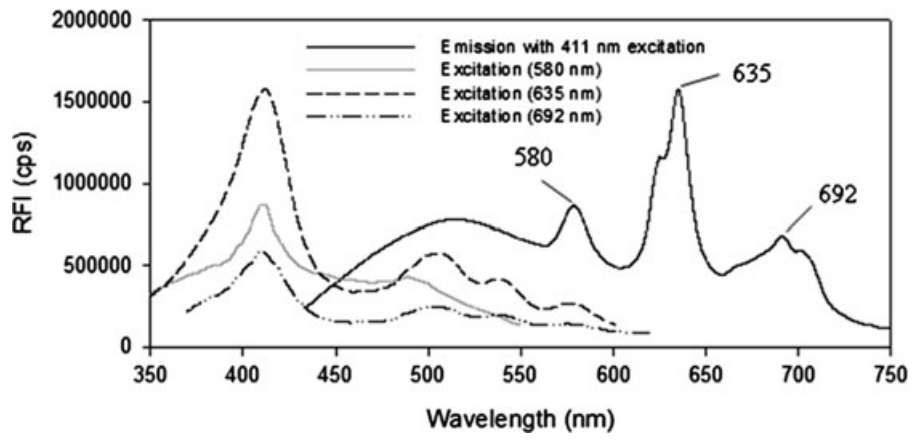

Figure 3—Representative fluorescence excitation and emission spectra of poultry fecal matter from ceca (Kim and others 2006).

the evidence of feces-treated spots on a poultry carcass, but the appearance of the feces spots on the poultry was time dependent. Within the time-resolved fluorescence images, 20- and 25-ns images exhibited relatively greater contrasts between the poultry skin and the feces spots. A detection delay-gate time between 20 and 25 ns may be suitable for the detection of feces contamination on poultry carcass.

F values of one-way ANOVA for RFI values of feces and skin across the gate-delay time were calculated and are shown in Figure 7A. A larger *F* value indicates a more statistically significant mean separation between the 2 groups. The result indicates that the mean of the 2 groups were most significantly separated by a delay-gate time at 22 ns. To find an optimal threshold value for separating feces from skin, classification accuracies were calculated for values across the RFI values. Results illustrated that the highest accuracy (96.6%) was obtained by using a threshold of 1120 RFI value (Figure 7B). As shown in the frequency histogram, the skin parts, the relatively low intensities, are largely grouped together in contrast to the wide spread of a higher intensities for the fecal matters.

On the basis of the discrimination analysis, undiluted and 1:5 diluted fecal matters could be detected with 100% accuracy regardless of feces types. Classification accuracy for 1:10 diluted feces with the dry matter contents of approximately 15 to 18 μg/g was 89.9%. Detection accuracies for ceca and colon (100% for both) were higher than those for small intestine and duodenum (90.8% and 95.8%, respectively). The fluorescence response of 1:50 diluted fecal matters could not be discriminated from skin; hence these were excluded from the analysis.

Figure 8 shows a sequence of processed images beginning with a photo of fecal matters placed on poultry skin. The fecal matters are arranged from top to bottom with no dilution in row 1, and with dilutions of 1:5, 1:10, and 1:50 in rows 2 to 4. The samples shown in columns 1 to 4 (from left to right) are fecal matters from the duodenum, small intestine, ceca, and colon, respectively. As shown in Figure 8A, the diluted fecal matters are not easily discernible by naked eye, except for those from ceca. Figure 8B is the image obtained from using a 22-ns gate-delay time after 5 × 5 binning. Scattered spots that have high fluorescence intensities were observed in the areas for skin. The binary-classification image was obtained by applying the 1120 RFI threshold value to the 22-ns gate-delay time image (Figure 8C). Portions of the highly diluted feces spots are missing, and a few false positives were observed in the sample areas for skin. To eliminate the false positives, a 2 × 1 erosion algorithm was applied. The resultant binary image showed the successful detection of fecal matters diluted up to 1:5 along with partial detection of 1:10 diluted fecal matters without false positive (Figure 8D).

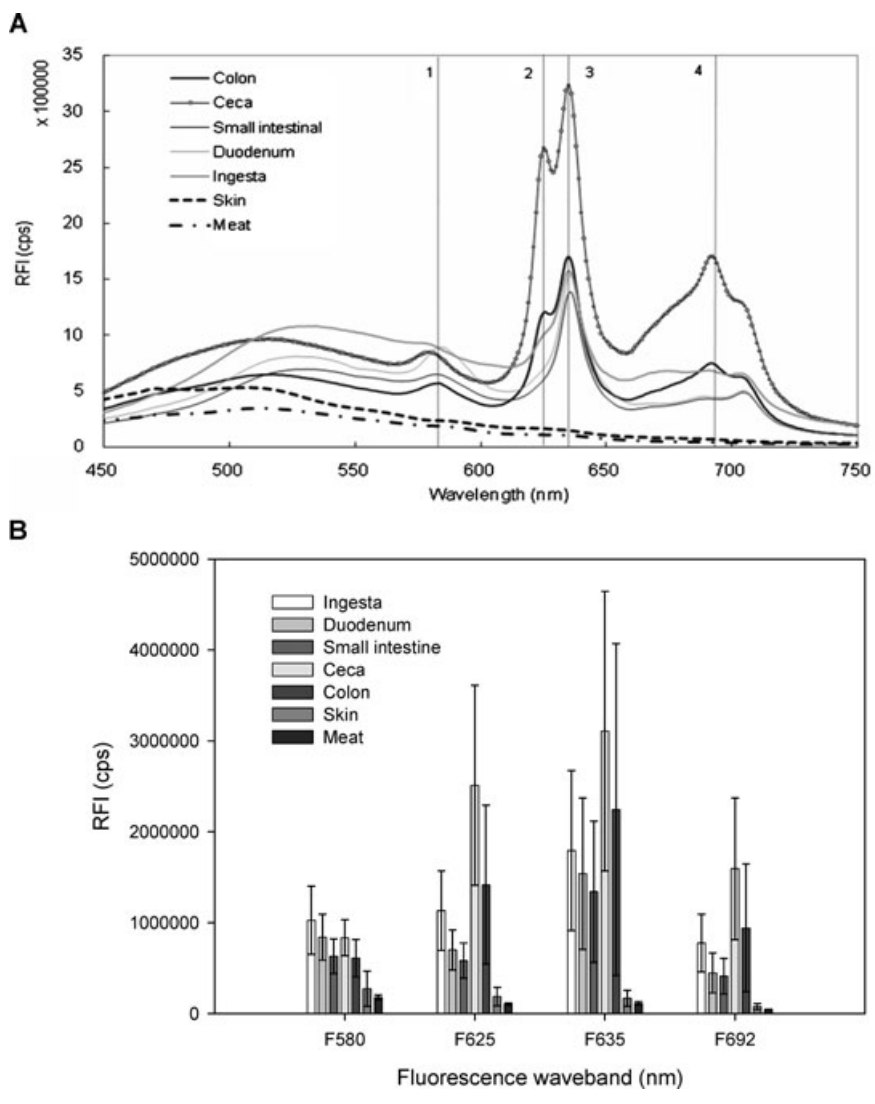

Figure 4—Representative mean spectra (A) and intensities (B) of poultry fecal matter at 580, 625, 635, and 692 nm. Error bars indicate standard deviations.

Conclusions

In this study, the optimization of imaging parameters of a LIFIS was investigated for the detection of diluted fecal matters applied to poultry skin. Fecal matters at dilutions as high as 1:10 could be detected with an accuracy of 96.6% using fluorescence emissions captured with the use of a 415-nm excitation source, 630-nm filter, and a 22-ns gate-delay time with an optimal threshold (for example, RFI 1120). The results demonstrate that the LIFIS has good potential for the detection of diluted feces on poultry carcasses and could be an alternative to the current human inspection method in automated poultry processing plants. To develop robust LIFIS for detecting various types and levels of diluted fecal contaminants, additional researches with more poultry carcasses fed by different feedstuff are warranted especially in an industrial setting.

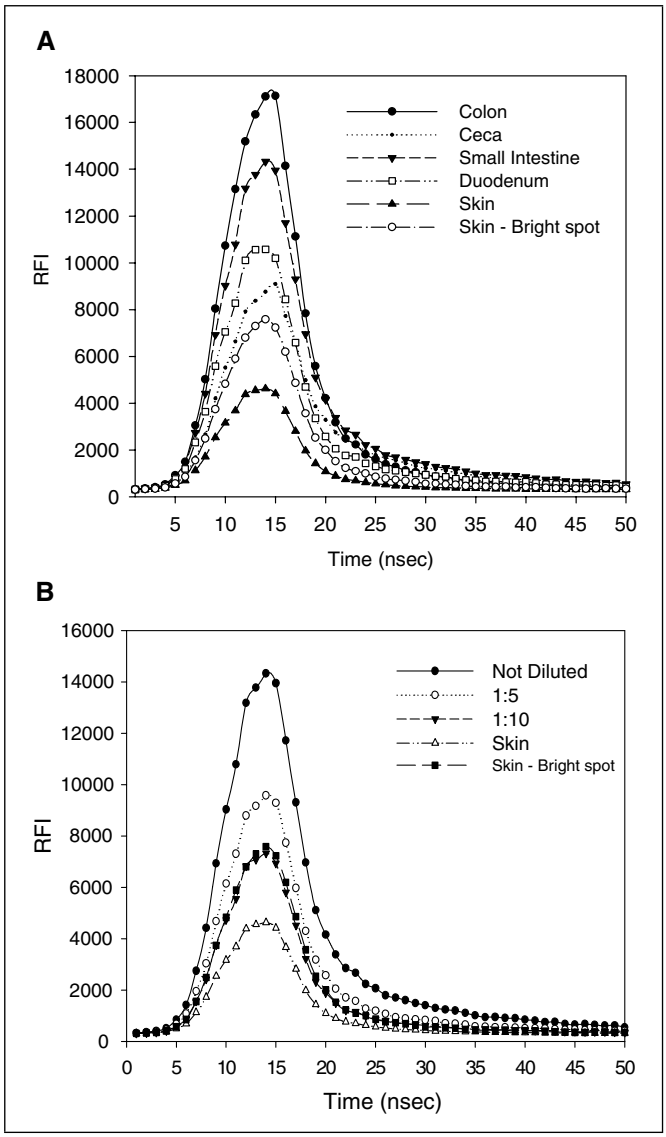

Figure 5—Representative time-resolved fluorescence emission spectra of poultry skin, and (A) undiluted and (B) diluted fecal matters.

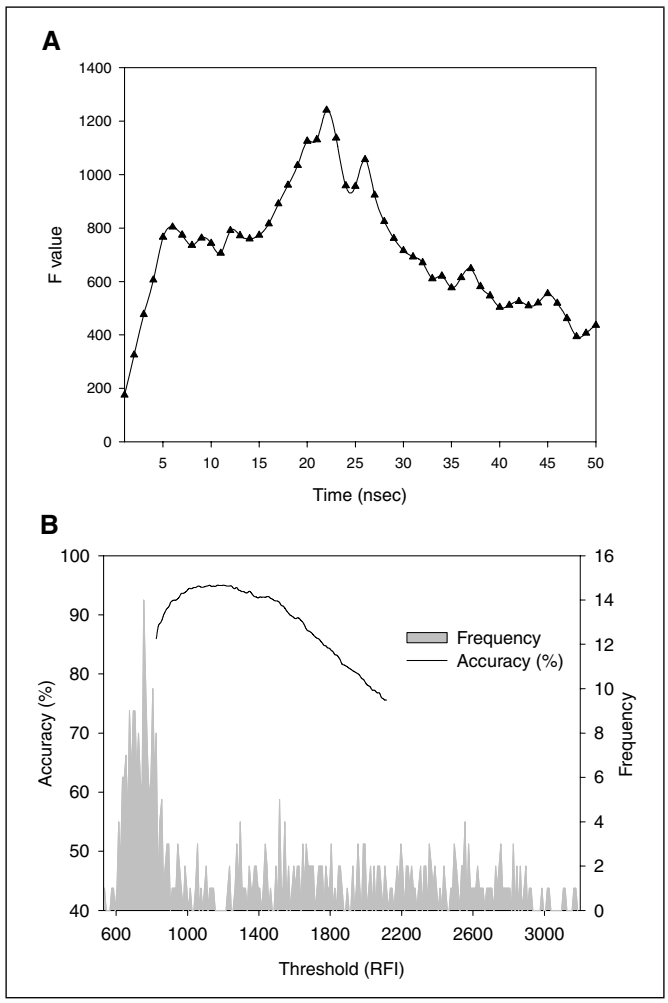

Figure 7—Gate-delay time and threshold value selection. (A) *F* values by delay-gate time used for classification, and (B) detection accuracy as a function of RFI threshold with frequency histogram for RFI values of feces and skin.

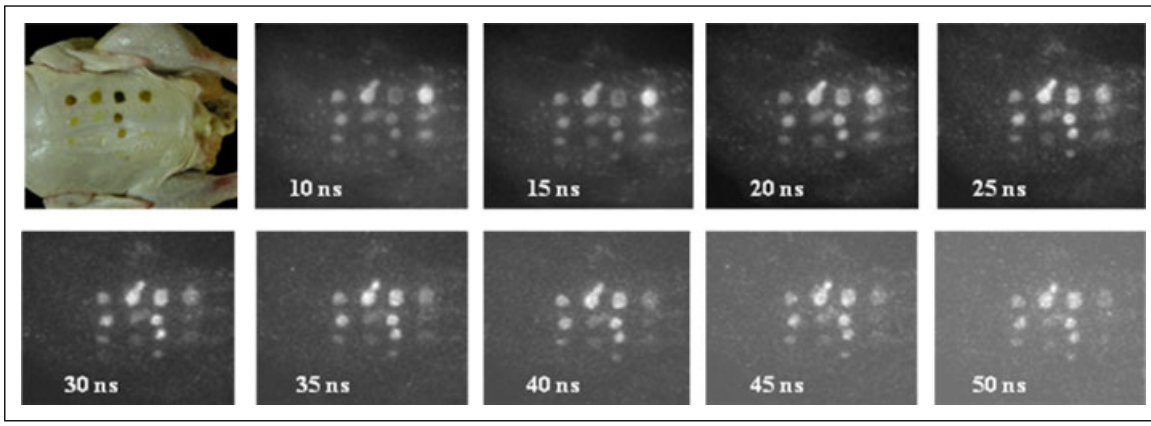

Figure 6—Time-resolved images at 630 nm spanning from 10 to 50 ns in 5-ns interval for a representative poultry artificially contaminated with the fecal dilutions, using 415-nm excitation.

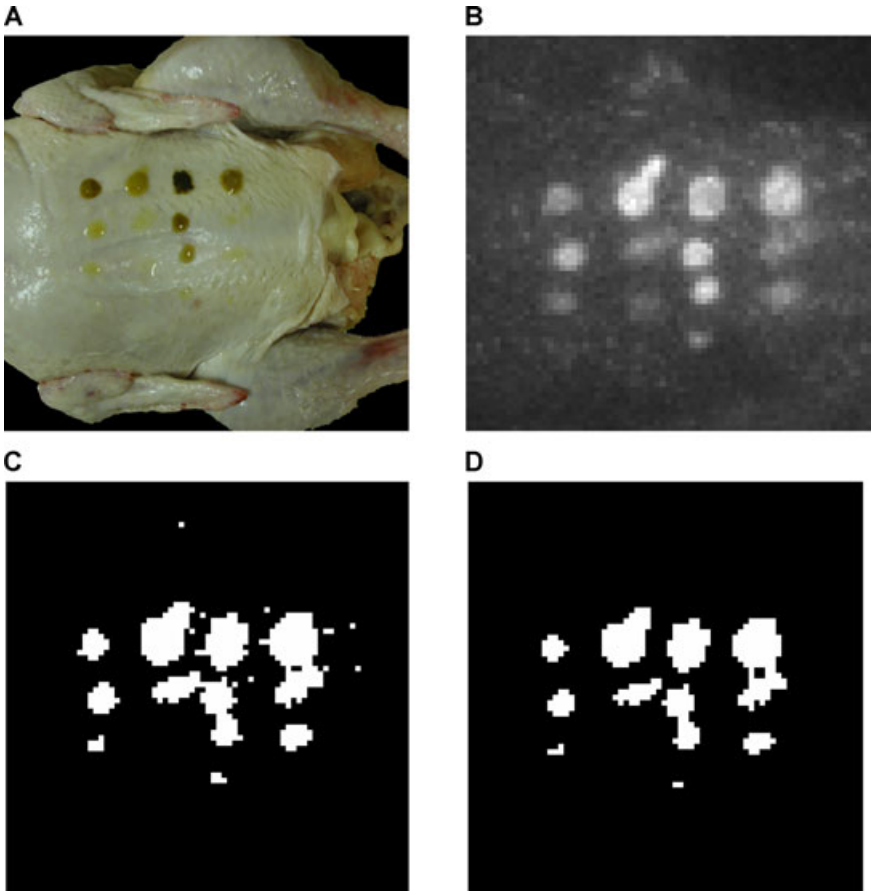

Figure 8—(A) Photo of contaminant on poultry skin; illustration of the image processing sequence: (B) 5 × 5 binned image at 22-ns gate-delay time, (C) binary image from a threshold of 1120 RFI, and (D) binary image with 2 × 1 image erosion.

Acknowledgments

This study was carried out with partial support of "Specific Joint Agricultural Research-promoting Projects (Project nr 20070301033004)," RDA, Republic of Korea.

References

Cody SH, Glynn MK, Farrar JA, Cairns KL, Griffin PM, Kobayashi J, Fyfe M, Hoffman R, King AS, Lewis JH, Swanminathan B, Bryant RG, Vugia DJ. 1999. An outbreak of *Escherichia coli* O157:H7 infection from unpasteurized commercial apple juice. Ann Int Med 130:202–9.

[FSIS] Food Safety and Inspection Service. 2004. Livestock post-mortem inspection activities-enforcing the zero-tolerances for fecal materials, ingesta, and milk. FSIS Directive:6420.2.

Mead PS, Slutsker L, Dietz V, McCaig LF, Bresee JS, Shapiro C, Griffin PM, Tauxe RV. 1999. Food-related illness and death in the United States. Emerg Infect Dis 5:607–25.

Kim MS, Lefcourt AM, Chen Y. 2003a. Multispectral laser-induced fluorescence imaging system for large biological samples. Appl Optics 42:3927–33.

Kim MS, Lefcourt AM, Chen Y. 2003b. Optimal fluorescence excitation and emission bands for detection of fecal contamination. J Food Prot 66:1198–207.

Kim MS, Cho B, Chao K, Lefcourt AM, Liu Y, Chen Y. 2006. Detection of contaminants on poultry processing plant equipment using laser-induced fluorescence imaging. Key Engr Matl 321-3:1157–62.

Kim MS, Cho B, Lefcourt AM, Chen Y, Kang S. 2008. Multispectral fluorescence lifetime imaging of feces contaminated apples by time-resolved laser-induced fluorescence imaging system with tunable excitation wavelengths. Appl Optics 47:1608–16.

Park B, Lawrence KC, Windham WR, Buhr RJ. 2002. Hyperspectral imaging for detection fecal and ingesta contaminations on poultry carcasses. T ASAE 45:2017–26.

Park B, Lawrence KC, Windham WR, Smith DP. 2005. Detection of cecal contaminations in visceral cavity of broiler carcasses using hyperspectral imaging. Appl Engr Agric 21:627–35.